Supporting Information

Three-Dimensional Blueprinting of Molecular Patterns in Liquid Crystalline Polymers

Mohsen Tabrizi,[a] J. Arul Clement,[a] Mahnoush Babaei,[c] Angel Martinez,[d] Junfeng Gao,[a] Taylor H. Ware,[b] and M. Ravi Shankar [a] *

[a] Department of Industrial Engineering, Swanson School of Engineering, University of Pittsburgh, PA 15261

[b] Department of Biomedical Engineering, Texas A&M University, 101 Bizzell Street, College Station, TX 77843

[c] Department of Aerospace Engineering & Engineering Mechanics, University of Texas at Austin, 2617 Wichita Street, C0600, Austin, TX 78712

[d] Department of Applied Physics and Materials Science, Northern Arizona University, Science Annex, 525 S Beaver St, Flagstaff, AZ 86011

* Corresponding Author (ravishm@pitt.edu)

Supplemental Figures

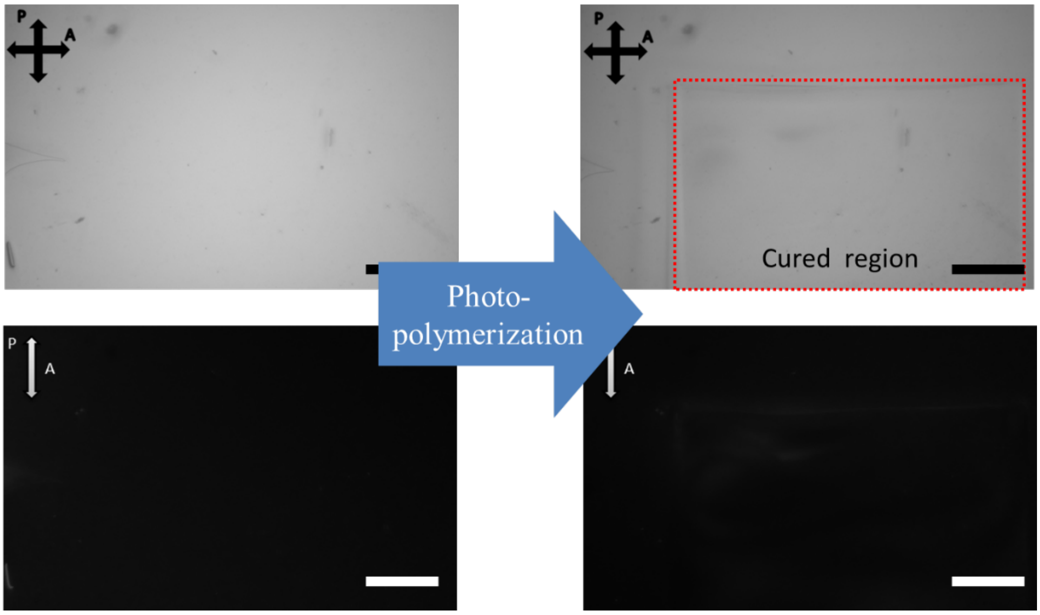

Figure S1. In-situ POM observations of the monomer pre- and post-polymerization with both parallel and crossed configurations of the polarizer (P) and analyzer (A) (scale bars = 1 mm).

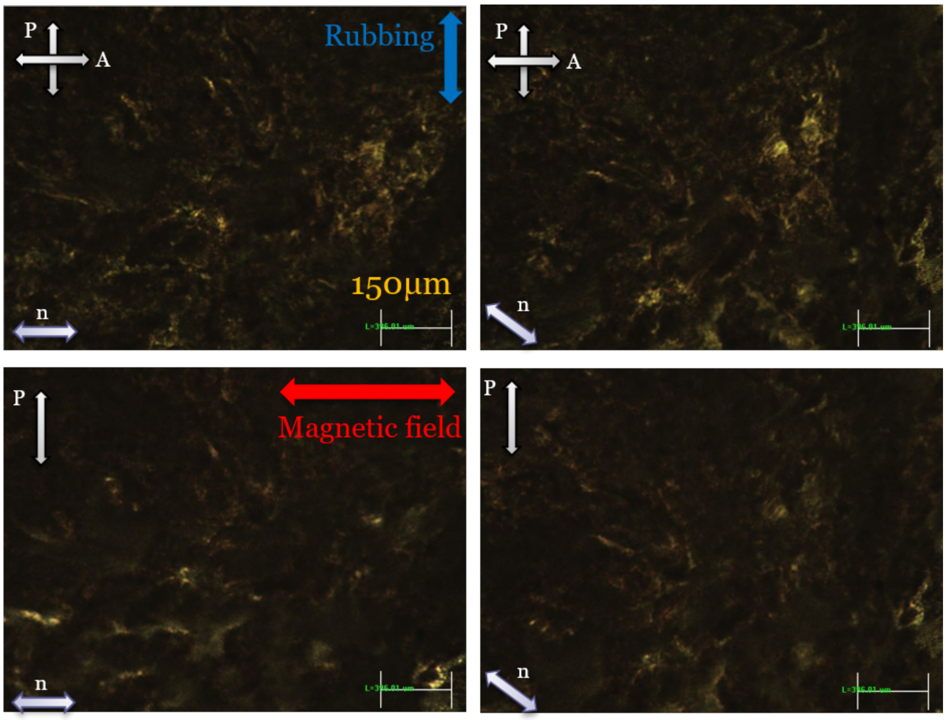

Figure S2. POM images of a 50 µm thick LCE prepared via a two-step Michael-addition method. The oligomeric material was fully polymerized at 55°C with a 300 mT external magnetic field. One side had strong surface anchoring using rubbed elvamide. The observations indicate that a 300 mT magnetic field, combined with elvamide anchoring, is insufficient to control molecular orientation through this method.

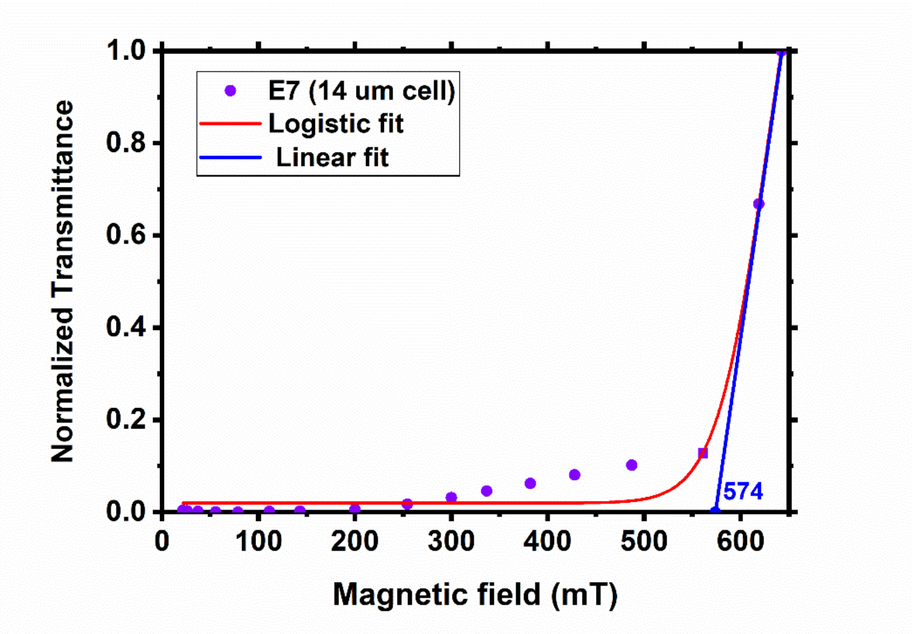

Figure S3. Plot of magnetic flux density vs. light transmission for the E7 monomer at room temperature. The red line represents the logistic fitting curves, while the blue line is derived from linear fitting to estimate the magnetic field threshold.

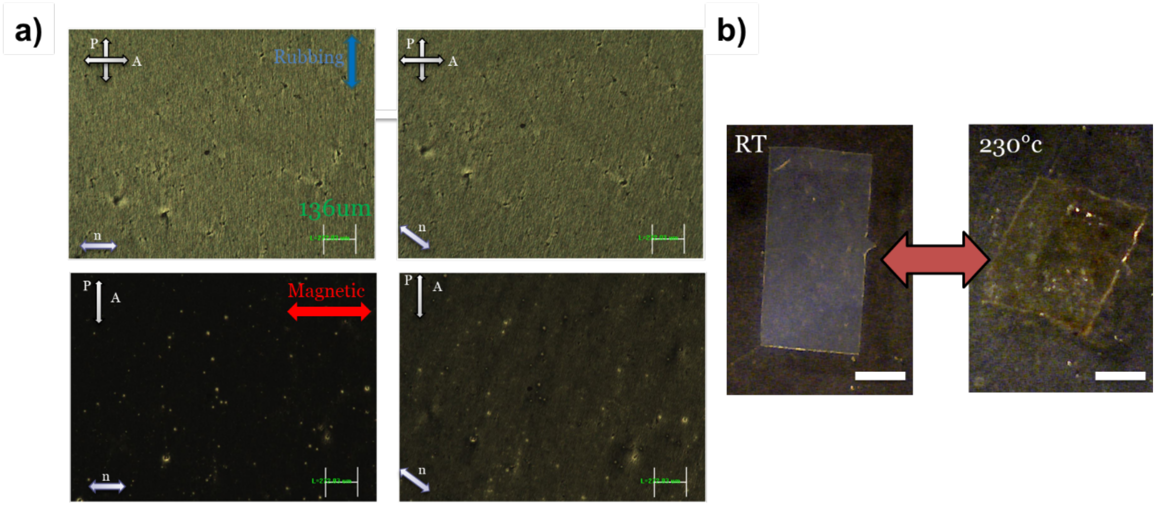

Figure S4. a) In-situ POM images of polymerized RMT10C3, displaying molecular order at 0° and 45° under both parallel and crossed configurations. b) Demonstration of a reversible 30% strain through thermal actuation (scale bars = 1 mm).

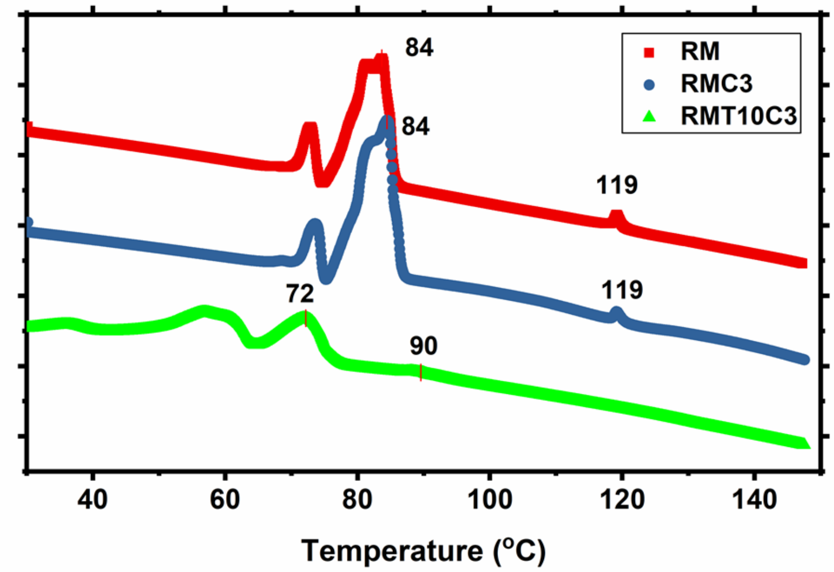

Figure S5. DSC curves illustrating the shift in phase transition temperatures upon the introduction of TBM and BDMT to the composition.

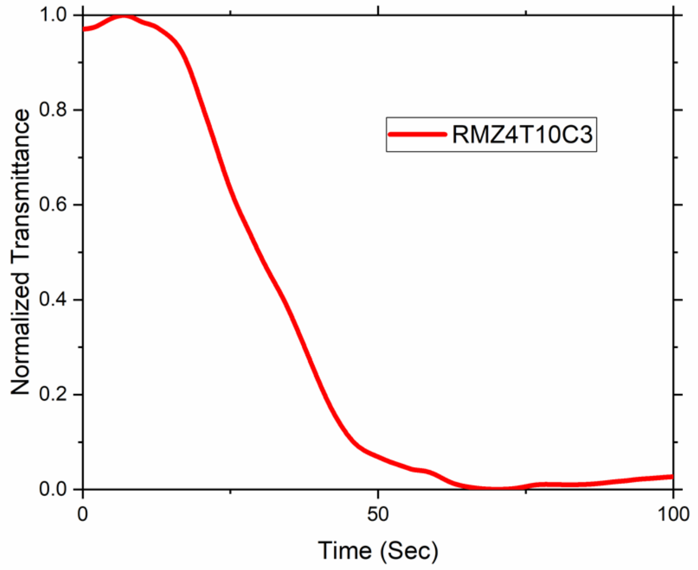

Figure S6. Drop in the transmission of polarized light through the material over time after the removal of the magnetic field, highlighting mesogens reorientation. This data specifically sheds light on the decay time and rate dynamics of magnetic alignment.

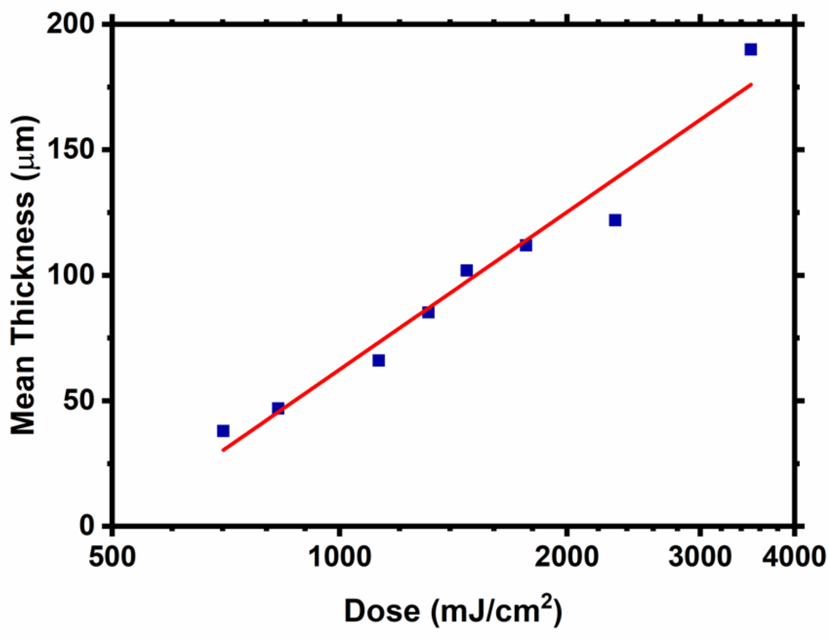

Figure S7. Working curve constructed to optimize control over polymerization depth. To collect data for this plot, the build-plate was positioned ~500 µm away from the window (fluorinated ethylene propylene: FEP film) to prevent it from constraining the polymerization depth. To control the dose, the exposure time was held constant, and the exposure intensity was adjusted by varying the grayscale patterns. Square-shaped patterns were exposed under these conditions and the thickness of the cured objects were subsequently measured after development and post-processing to determine the polymerization depth for each dose. The experiment was conducted three times for each data point to characterize the repeatability.

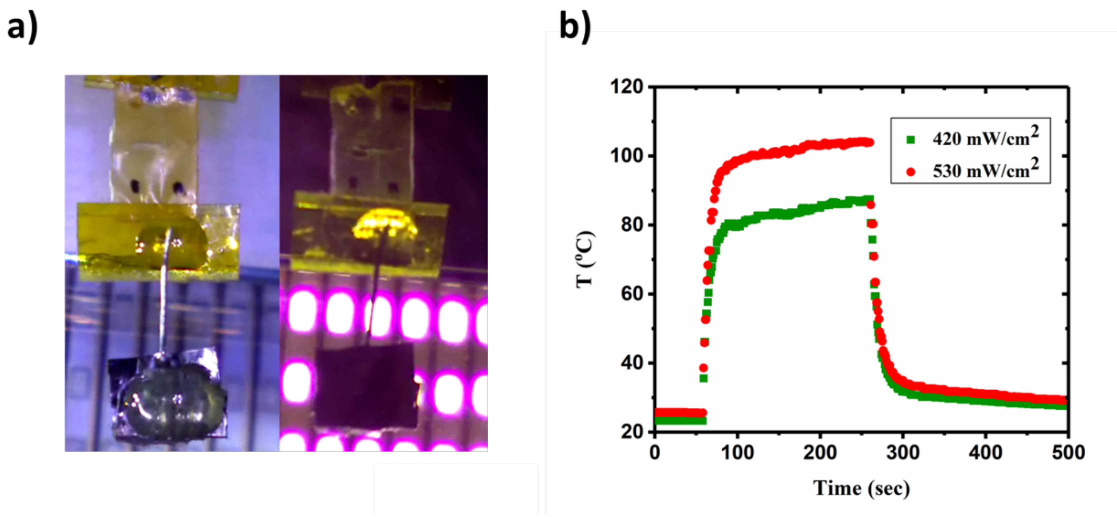

Figure S8. a) Image of the weight lifting setup where the magnetically aligned LCE film lifts a 10mg weight in response to UV light exposure. b) Illustration of the photothermal effect at two different light intensities: 420 mW/cm^2 and 530 mW/cm^2.

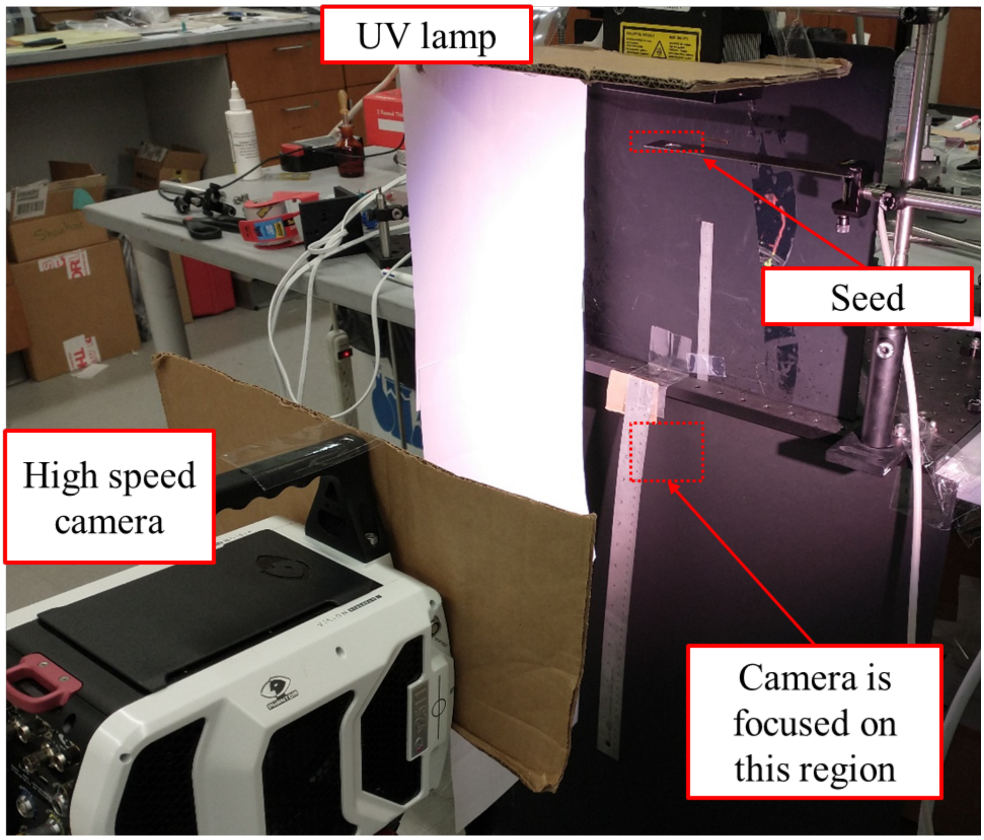

Figure S9. Imaging setup to analyze the flight dynamics of the printed LCE microflier. After 1 minute of UV exposure, the microflier was released from the sample location and its descent, 25 cm from the drop point, was captured using a high-speed video camera at a rate of 5000 fps.

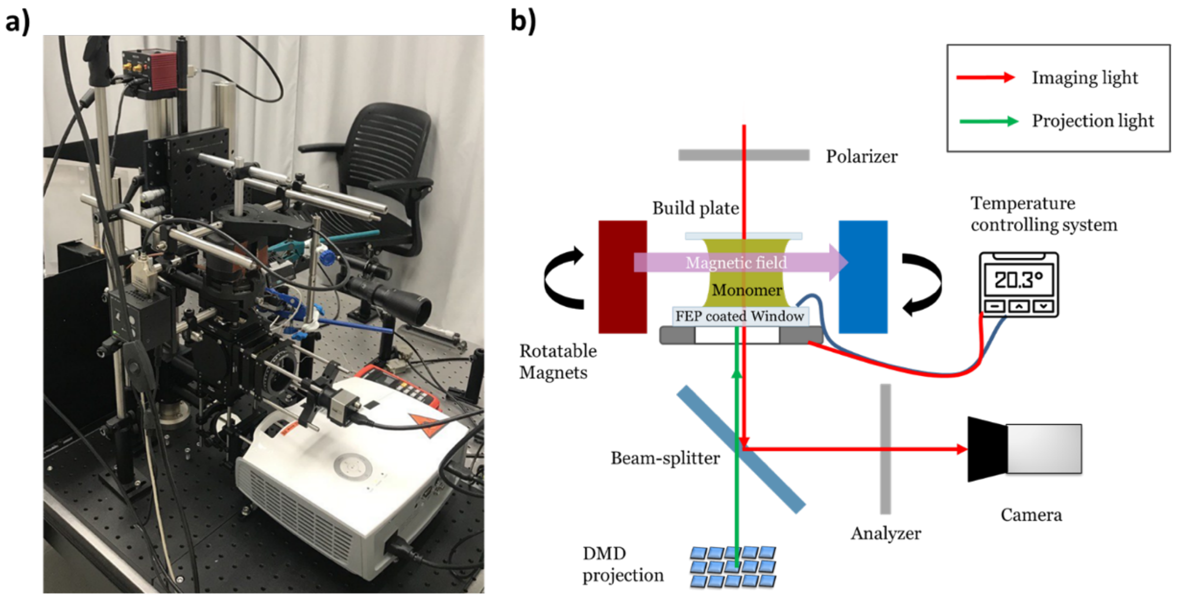

Figure S10. a) The 3D printer setup capable of programming the mesogens orientations voxel-by-voxel b) Schematic representation of the printing process accompanied by in situ observation.

The 300 mT magnetic field was generated by firmly mounting two Neodymium Block Magnets (1 1/2" x 1 1/2" x 3/4" N52, K&J Magnetics) with a 30 mm separation onto a motorized rotation stage (PRM1Z8, Thorlabs). The temperature of the build zone was controlled using a PID controller that utilized a self-adhesive thermocouple (SA3-K, Omega). The projected pattern from the DMD (D912HD, Vivitek) was transmitted toward the window through a Thorlabs cage system (LC6W) equipped with mirror, lenses, iris, UV filter (for green light exposure), and a beam splitter. For imaging purposes, polarized red light was used to prevent unintended photopolymerization during imaging. The light was reflected by the beam splitter and passes through the analyzer toward the camera. Further details of this setup can be found in Ref. 13 of the manuscript.

Movies

Movie S1. Reversible photoactuation of microflier demonstrating the change in the profile of the samara (wing).